

# FABRICATION OF NB / AL-N<sub>x</sub> / NBTiN JUNCTIONS FOR SIS MIXER APPLICATIONS ABOVE 1 THZ

B. Bumble, H. G. LeDuc, and J. A. Stern  
Center for Space Microelectronics Technology, Jet Propulsion Laboratory,  
California Institute of Technology, Pasadena, CA 91109, USA

## ABSTRACT

We discuss the material processing limits of superconductor-insulator-superconductor (SIS) junctions with an energy gap high enough to enable THz heterodyne mixer detection. The focus of this work is a device structure which has Nb as a base layer, a tunnel barrier formed by plasma nitridation of a thin Al proximity layer, and NbTiN as a counter-electrode material. These SIS junctions typically exhibit 3.5 mV sum-gap voltages with the sub-gap to normal state resistance ratio  $R_{sg} / R_N = 15$  for resistance - area products  $R_N A = 20 \Omega \mu\text{m}^2$ . This process is developed such that junctions will be integrated to mixer antenna structures incorporating NbTiN as both ground plane and wire circuit layers. Run-to-run reproducibility and control of the  $R_N A$  product is addressed with regard to the conditions applied during plasma nitridation of the Al layer. RF plasma nitridation of the aluminum is investigated by control of DC floating potential,  $N_2$  pressure, and exposure time. Processing is done at near room temperature to reduce the number of variables. Stress in the metal film layers is kept in the low compressive range. Recent receiver results will be discussed in another work presented at this symposium. [1]

## INTRODUCTION

High quality Nb/Al-Ox/Nb Josephson junctions have produced the lowest noise temperatures in heterodyne receivers up to 1 THz.[2] Low noise temperatures have been achieved above the energy gap frequency of Nb ( $2\Delta/h \sim 700\text{GHz}$ ) by using high conductivity normal metal (Al) tuning circuits. However, the ideal superconductor-insulator-superconductor (SIS) junction for THz heterodyne receivers should incorporate a high transition temperature ( $T_c$ ), low-loss superconductor. Applications of tunnel junctions fabricated with NbN/ MgO/NbN and NbN/AlN/NbN have been reported, but performance seems to be limited by either gap rounding in the current- voltage (I-V) characteristic or surface resistance in the NbN. [3,4]. Thin films of NbTiN used in RF accelerator cavities have shown an improvement in surface resistance over NbN.[5] Recent measurements from mixers fabricated with NbTiN have shown that losses can be quite low. [6] However, the integration of Nb/Al-Ox/Nb junctions with NbTiN ground planes and wires suffers from gap reduction due to quasiparticle trapping at the Nb/NbTiN interfaces on both sides of the junction. There is also a problem with getting an insulator - NbTiN interface clean enough such that the superconducting energy gap does not degrade over the distance of its coherence length. Junctions which have deposited

barrier layers are prone to tunneling irregularities due to thin spots or “pin-holes.” Transmission electron microscope (TEM) images of Nb/Al-Ox/Nb junctions clearly show that aluminum smoothes out over the granular niobium surface. [7] Thermal oxidation of the aluminum surface produces a dense and uniform insulator. The niobium counter-electrode may degrade slightly at the interface, but not over the distance of its relatively long coherence length.

Below is a table of the enthalpy of formation for some compounds of interest for this work: [8] The information is useful in that it helps to predict the direction of surface reactions which may occur. Note that the oxides tend to be more stable than the nitrides. Thus, excess oxygen on an Al<sub>2</sub>O<sub>3</sub> surface will tend to react with a deposited NbTiN layer to degrade the superconductor at the interface. Depositing NbTiN on a layer of AlN should have less of an ill effect on the superconductor. However, depositing pure Al on a NbTiN base depletes the superconductor of nitrogen at the interface. We also want to point out that thermal oxidation of Al is much easier than thermal nitridation because the triple bond of N<sub>2</sub> is harder to break than the double bond in O<sub>2</sub>. Producing a nitride requires either higher temperatures or creating a plasma to break the N<sub>2</sub> molecule. Another method is to get free nitrogen from a gas such as NH<sub>3</sub> which is more reactive.

Compound	ΔH (Kcal/mol)
AlN	-76
NbN	-56
Al <sub>2</sub> O <sub>3</sub>	-401
Nb <sub>2</sub> O <sub>5</sub>	-454
N element	+113
O element	+60
NH <sub>3</sub>	-11

Figure 1. Heats of Formation

The work presented here deals only with plasma nitridation at near room temperature by driving the substrate with an RF generator. AlN is an insulator of similar properties to Al<sub>2</sub>O<sub>3</sub> with band gap energy ~4 eV and dielectric constant of 8.5. [8] Nb/Al-Nx/Nb Josephson junctions produced by plasma nitridation of aluminum have been previously investigated by Shiota, et al and shown to exhibit improved annealing stability over oxide barriers. [10] Replacing the counter-electrode with NbTiN has the advantage of moving the sum-gap voltage out by 0.6 mV. Thus, a THz receiver would have a substantial improvement in bias range. Figure 2 shows a comparison of a

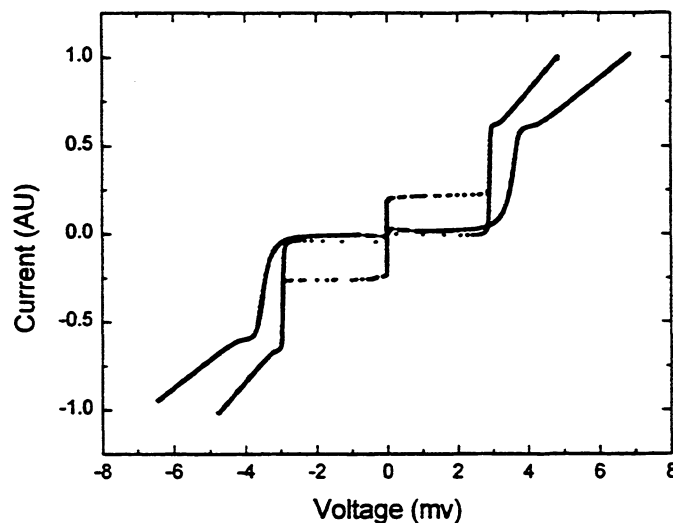


Figure 2. Nb/Al-Ox/Nb compared to Nb/Al-Nx/NbTiN

Nb/AlO<sub>x</sub>/Nb junction with 2.9 mV gap to a Nb/Al-N<sub>x</sub>/NbTiN junction with 3.5mV gap. Both junctions have  $R_{N,A} \sim 20 \Omega\text{-}\mu\text{m}^2$  and are plotted with arbitrary units for the current scale so that the gap voltages and step features can be compared.

### EXPERIMENTAL TECHNIQUE

Junctions for this set of experiments are fabricated by a trilayer deposition and self-aligned processing technique. Details of the pattern and etch steps of this technique are reported in another paper in these proceedings.[11] The point of focus presented here is on trilayer deposition which involves plasma nitridation of the Al proximity layer. A brief description and illustration of the process steps for trilayer deposition are given below:

1. DC magnetron sputter deposition of 150 nm of Nb.
2. DC magnetron sputter deposition of 7 nm of Al.
3. Growth of nitride barrier using pure N<sub>2</sub> plasma exposure of Al layer.
4. DC magnetron reactive sputtering 50 nm NbTiN in Ar + N<sub>2</sub> gas mixture.

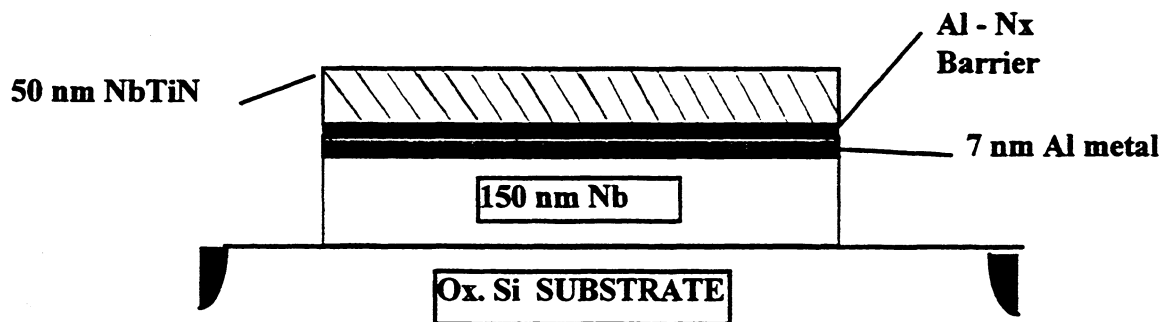


Figure 3. Diagram of Nb/Al-N<sub>x</sub>/NbTiN layered structure as studied.

Our process development is investigated for two separate vacuum systems. We have produced devices for receiver testing in system #1 and are currently attempting to transfer the process to system #2. Although the two cylindrical chambers are similar in many respects, system #1 is 46 cm in diameter and 36 cm high whereas system #2 is 76 cm in diameter and 48 cm high. Sputtering sources are all DC magnetrons with 7.6 cm diameter targets which are positioned to sputter upward with a target to substrate throw distance of about 6 cm. Samples are inserted through a vacuum load-lock chamber. A manipulator arm rotates about the chamber center to place the sample over the various sources located around the circumference. All depositions are done without extra heating such that substrate temperature is between 30-60 °C. Samples are held on a metal platform which is grounded for all process steps except the plasma nitridation.

Trilayers are deposited in-situ with a base pressure lower than  $10^{-5}$  Pa. Substrates used in this experiment were thermally oxidized Si wafers. They were cleaned in-situ

prior to film deposit with mild Ar ion beam exposure of 150eV, 20mA for 45 seconds in system #2 and Ar plasma cleaned with comparable conditions in system #1. The base layer of Nb is deposited under sputter conditions which produce slight compressive stress in the film of  $2-5 \times 10^9$  dynes/cm<sup>2</sup>. Typical deposition rates are 50 nm/min. in 10 mTorr Ar ambient. These conditions have resulted in the best results for Nb/Al-Ox/Nb junctions and we have seen indications that it is desirable for junctions with subsequent nitride layers as well.

The aluminum layers are deposited by oscillating the sample over the target such that a 7 nm thick film is grown with about 75 passes for system #1 and about 10 passes for system #2. This method produces a more uniform thickness distribution than by remaining stationary over the target.

Plasma nitridation of the aluminum layer is done at a chamber location which allows about 15 cm of free space between the wafer face and the grounded chamber bottom. The substrate manipulator is a grounded cylindrical assembly with capabilities for 13 MHz RF biasing of the bottom chuck which the substrate is held to. Nitrogen gas of 99.999 % purity is flowed into the chamber at ~10 sccm and the pressure is controlled by throttling a turbomolecular pump. RF power of less than 10 W is applied through an impedance matching network to the substrate platform. The DC floating potential developed on the substrate is feedback controlled for the required exposure time.

Counter-electrode deposition of 50 nm thick NbTiN is done by reactive DC magnetron sputtering from a Nb<sub>78</sub> Ti<sub>22</sub> (wt. %) target in an ambient of Ar and N<sub>2</sub>. The flow ratio for optimum properties of NbTiN is integrally related to deposition rate, total gas pressure, target and substrate temperature, and plasma dynamics which involve fixture geometry. Furthermore, there is a compromise to be made between the properties of film stress, T<sub>c</sub>, and resistivity. Typical values for films in this study are T<sub>c</sub> = 14-15 K,  $\rho_{20K} = 75-85 \mu \Omega \text{ cm}$ , and compressive stress ( $\sigma$ ) =  $5-10 \times 10^9$  dynes/cm<sup>2</sup>. A more detailed description of the NbTiN film deposition process is given in a separate paper in these proceedings. [11]

## PROCESS VARIATIONS AND RESULTS

Junctions are characterized by low frequency electrical testing in liquid He at near 4.2 K in temperature. Test chips each have 12 various sized square junctions with side dimensions on the lithography mask designed from 0.8  $\mu\text{m}$  up to 5  $\mu\text{m}$ . We have chosen to use the parameter  $R_N A$  (product of normal state resistance and junction area) rather than current density because this value is derived by statistically fitting the measured  $R_N$  with the junction dimensions. Since the gap voltage ( $V_g$ ) is typically 3.5 mV, current density ( $J_c$ ) can be calculated by the Ambegaokar-Baratoff relation  $J_c R_N A = \pi V_g / 4$ . [12]

**a. Bias variation**

Figure 4 is a plot of junction  $R_N A$  product for DC floating potential values ranging from -35 to -80 V. This data only exists for system #2 at the present time. The background nitrogen pressure is held constant at 20 mTorr and exposure time is between 1-2 minutes. Corresponding junction quality is also plotted as the ratio of sub-gap resistance at 2 mV to normal state resistance ( $R_{sg}/R_N$ ). Increasing the floating potential means that both ion energy and density will be increased. The  $R_N A$  value does increase and it is inferred that AlN thickness grows faster by increasing bias. Junction quality ( $R_{sg}/R_N$ ) improves up to the point near 75eV where sputtering thresholds cause surface damage. The  $R_N A$  values presented in Figure 4 are rather low, therefore, this apparent improvement could also simply result from reducing “pin-hole” density as the AlN<sub>x</sub> grows.

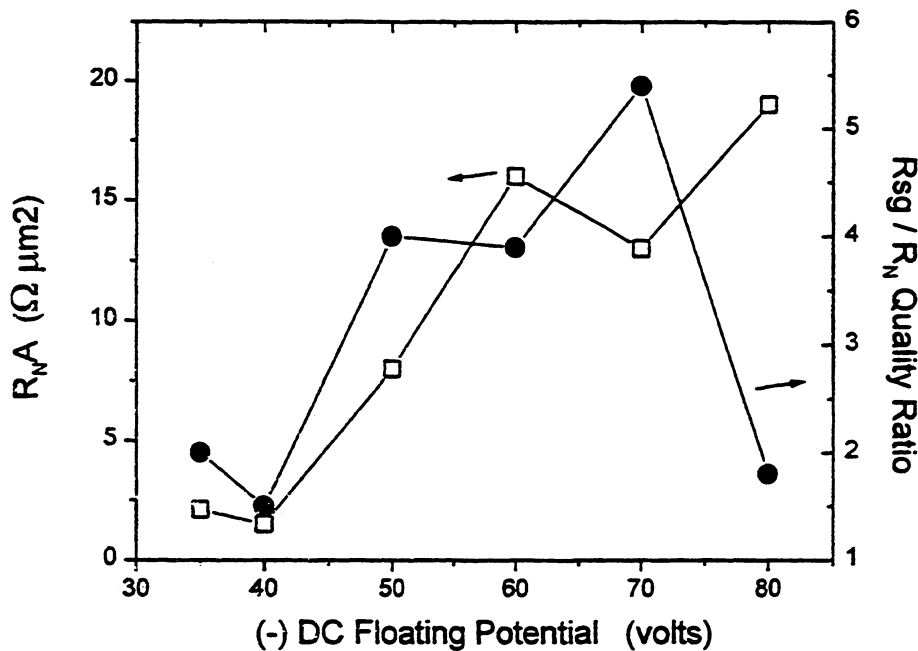


Figure 4. (□)  $R_N A$  and corresponding (●)  $R_{sg}/R_N$  as bias voltage is varied. 1-2 minutes at 20mTorr  $N_2$  in System #2

### b. Exposure time

We also investigated the effect of the duration of plasma exposure as a control parameter for  $R_{N}A$ . Figure 5 shows how  $R_{N}A$  varies with exposure times from 30seconds up to 5 minutes for two different vacuum systems. Nitrogen pressure is again held at 20 mTorr for both systems. DC floating potential is held at -35V for system #1 and -25V for system #2. Lines are drawn to guide the eye only. Data for system #1 seems to show a higher rate of  $AlN_x$  formation than for system #2. Both systems were driven by low energy plasmas, but the substrates did come out of system #1 at a hotter temperature. Scatter in the data for 60 second exposure times demonstrates the difficulty with run-to run reproducibility. Corresponding  $R_{sg}/R_N$  is not plotted, but it should be noted our highest quality junctions ( $R_{sg}/R_N \sim 20$ ) were produced with exposures between 1 to 2 minutes in system #1.

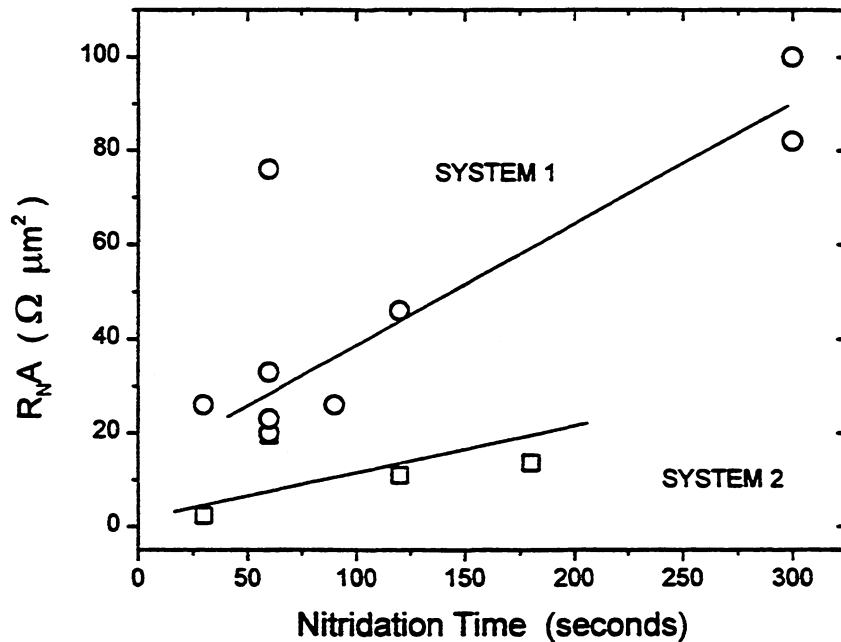


Figure 5. Junction  $R_{N}A$  vs plasma exposure time for (o) system #1 and (□) system #2, 20mTorr  $N_2$  and approximately -30V.

### c. N<sub>2</sub> Pressure variation

Figure 6 demonstrates the result of nitrogen pressure variation between 5 to 25 mTorr for system #1 and between 20 to 40 mTorr for system #2.. Pressure ranges were determined by plasma constraints and a desire for  $R_{NA}$  values near  $20 \Omega \mu\text{m}^2$ . Here the DC floating potential is held constant at approximately -30V and exposure time is fixed to 1 minute since those conditions seemed to be optimum from previous data sets for the current density of interest.  $R_{NA}$  is presented on a logarithmic scale because of its range. Data for system #1 is inconclusive since there is so much scatter, but data for system #2 does exhibit a trend between 25-37 mTorr. A value at 35 mTorr was reproduced once. Here the general trend of increasing  $R_{NA}$  with nitrogen pressure is expected thermodynamically since the nitride growth should increase with pressure.

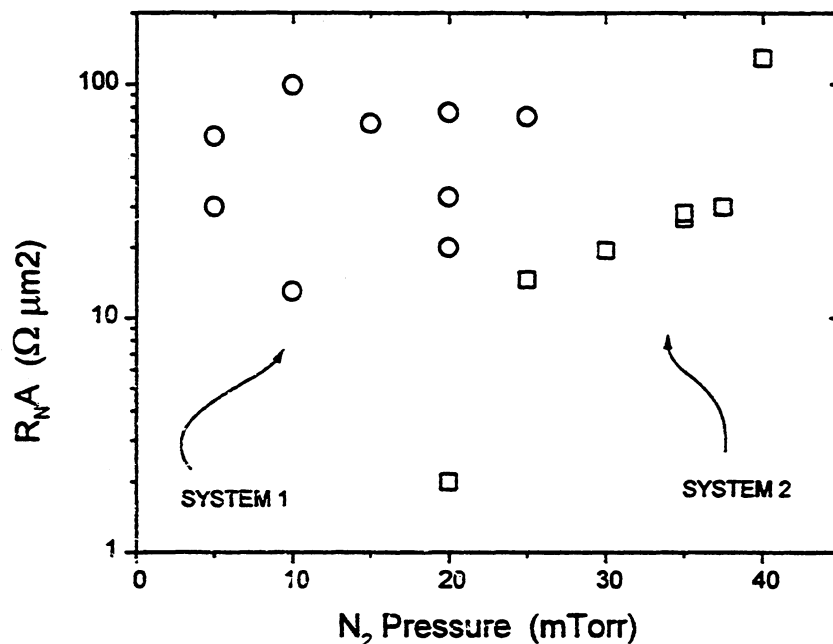


Figure 6. N<sub>2</sub> pressure effect on RNA product for (o) system #1 and (□) system #2 60second exposure, approximately -30V.

#### d. Junction quality

Quality of junctions produced under many different nitridation conditions is plotted in Figure 7 as the resistance ratio  $R_{sg}/R_N$  against junction  $R_N A$  product. Most of the data for both vacuum systems is clustered around  $R_N A = 20 \Omega \mu m^2$  since that is the current design target for mixer applications. Values plotted for  $R_{sg}/R_N$  are obtained from statistics on 10 or more junctions of the size range given above which do not have extraneous processing flaws. System #1 produced the best junctions with the highest average ratio of 18 for  $R_N A = 69 \Omega \mu m^2$ . Larger  $R_N A$  junctions may show higher quality, but processing is not optimized around high  $R_N A$  in this set of experiments. System #2 has never produced a junction with  $R_{sg}/R_N$  above about 10. There is a trend exhibited in both systems to rapidly change junction quality in the range between 10 to  $30 \Omega \mu m^2$ . Junctions down to  $4 \Omega \mu m^2$  have been made with resistance ratio of more than 5.

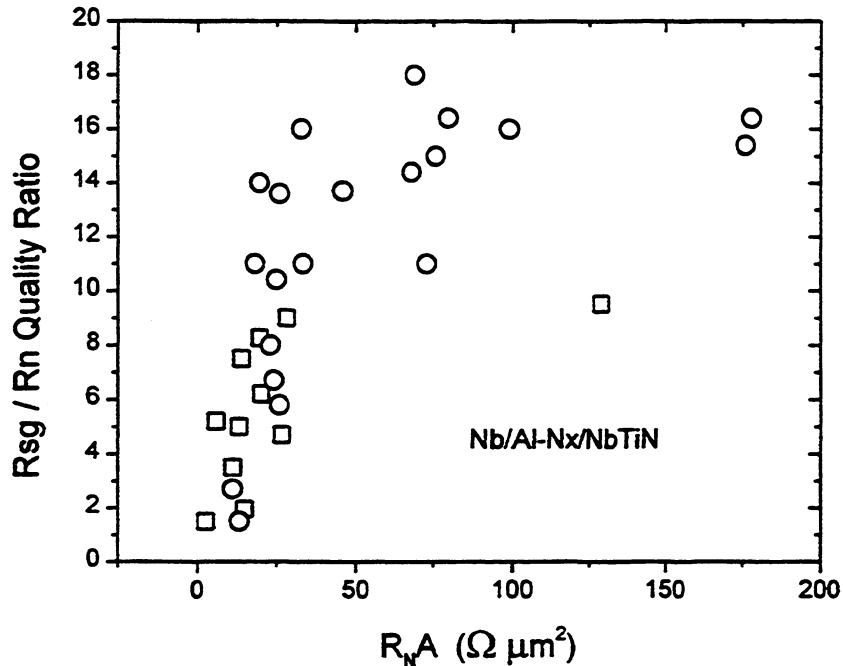


Figure 7. Resistance ratio vs  $R_N A$  for (o) system #1 and (□) system #2 for various RF plasma nitridation conditions.



## CONCLUSIONS

We have presented our results from process development of Nb/Al-N<sub>x</sub>/NbTiN junctions which is focused on RF plasma nitridation of the aluminum proximity layer. System #1 is shown to produce the higher quality junctions, but system #2 seems to have more controllable and reproducible results. SIS mixers with  $R_{N/A} = 20 \Omega \mu\text{m}^2$  and resistance ratios of 15 can be fabricated by this method if run-to-run variations are acceptable. Other experimental data on temperature control are needed. It is anticipated that nitride junctions will benefit from higher temperature processing because of improvement in the NbTiN quality, but there is still a question of control for  $R_{N/A}$  values of interest. Another avenue of investigation is to thermally nitride the aluminum with NH<sub>3</sub>. We think that the voltage gap of 3.5mV will bring a significant improvement in bias range for THz SIS receivers. Low noise temperatures should result from low-loss NbTiN tuning circuits combined with the junction's sharp I-V behavior.

## ACKNOWLEDGEMENTS

This research was performed by the Center for Space Microelectronics Technology, Jet Propulsion Laboratory, California Institute of Technology, and was sponsored by the National Aeronautics and Space Administration, the Office of Space Science.

## REFERENCES

- [1] J.W. Kooi, J.A. Stern, G. Chattadpadhyay, H.G. LeDuc, B. Bumble, and J. Zmuidzinas, "Low-loss NbTiN films for THz SIS mixer tuning circuits," *Int. J. IR and MM Waves* **19**, 1998 (in press).
- [2] M. Bin, M.C. Gaidis, J. Zmuidzinas, T.G. Phillips, and H.G. LeDuc, "Low-noise 1 THz niobium superconducting tunnel junction mixer with normal metal tuning circuit," *Appl. Phys. Lett.* **68**, pp.1714-1716, 1996.
- [3] A. Karpov, B. Plather, and J. Blondel, "Noise and gain in frequency mixers with NbN SIS junctions," *IEEE Trans. Applied Superconductivity* **7**, pp.1077-1080, 1997.
- [4] Z. Wang, A. Kawakami, Y. Uzawa, and B. Komiyama, "High critical current density NbN/AlN/NbN tunnel junctions fabricated on ambient temperature MgO substrates," *Appl. Phys. Lett.* **64**, pp. 2034-2036, 1994
- [5] R. Di Leo, A. Nigro, G. Nobile, and R. Vaglio, "Niobium- titanium nitride thin films for superconducting rf accelerator cavities," *J. Low Temp. Phys.* **78**, pp. 41-50, 1990

- [6] J. Zmuidzinas, J. Kooi, J. Kawamura, G. Chattopadhyay, B. Bumble, H.G.LeDuc, J.A. Stern, "Development of SIS mixers for 1 THz," Proceedings of SPIE (to be published), 1998.
- [7]] T. Imamura and S.Hasuo, "Cross-sectional TEM observation of Nb/Al-Ox - Al/Nb Junction structures," IEEE Trans. Mag. **27**, No.2, pp.3172-3175, 1991.
- [8] O.Kubaschwski and C.B. Alcock, *Metalurgical Thermochemistry*, 5<sup>th</sup> Ed., Pergamon Press, 1979.
- [9] G. Lewicki and C.A. Mead, "Currents through thin films of aluminum nitride," J. Phys. Chem. Solids **29**,pp.1255-1267, 1968.
- [10] T. Shiota, T. Imamura, and S. Hasuo, "Nb Josephon junction with an AlN<sub>x</sub> barrier made by plasma nitridation," Appl. Phys. Lett. **61**, pp. 1228-1230, 1992.
- [11] J. Stern, B. Bumble, H. LeDuc, "Fabrication and DC characterization of mixers for use between 600 and 1200 GHz," ( these proceedings)
- [12] Ambegakor and A. Baratoff,. "Tunneling between superconductors," Phys. Rev Lett. **10**, pp. 486-491, 1963.